Showcasing research from Professor Renwu Zhou's laboratory, School of Electrical Engineering, Xi'an Jiaotong University, Xi'an, China

Lightning-driven plasma bubbles provide prebiotic synthesis and biogeochemical cycling

The prebiotic synthesis of life molecules has always been a crucial process in the origin of life. This study proposes for the first time that the plasma bubbles formed by lightning strikes on a liquid surface can simultaneously synthesize various life molecules, such as amino acids and bases. These bubbles may serve as a potential "cradle" for the evolution of life molecules.

Image reproduced by permission of Renwu Zhou from *Chem. Commun.*, 2026, **62**, 2558.

As featured in:

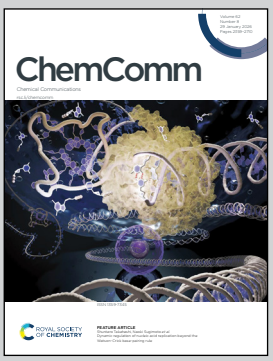

See Tianqi Zhang, Jianxi Ying, Renwu Zhou *et al.*, *Chem. Commun.*, 2026, **62**, 2558.

ROYAL SOCIETY OF CHEMISTRY

rsc.li/chemcomm

Registered charity number: 207890

ChemComm

COMMUNICATION

View Article Online
View Journal | View Issue

Cite this: *Chem. Commun.*, 2026, **62**, 2558

Received 29th July 2025,
Accepted 8th December 2025

DOI: 10.1039/d5cc04325e

rsc.li/chemcomm

Lightning-driven plasma bubbles provide prebiotic synthesis and biogeochemical cycling

Dingwei Gan,[a] Longfei Hong,[a] Xiaofan Guo,[b] Haoxuan Jiang,[a] Santu Luo,[a] Tianqi Zhang,*[c] Jianxi Ying,*[b] Rusen Zhou,[a] Dingxin Liu,[a] H. James Cleaves,[d] Yufen Zhao[b] and Renwu Zhou*[a]

Lightning–sea interactions generate plasma bubbles that act as electrochemical reactors, producing amino acids, nucleobases, and peptides with yields 100–300% higher than spark discharges. This process accelerates carbon-nitrogen coupling and enhances biogeochemical cycling, linking CO_2 and NH_3 to bioavailable organic compounds.

The origin of life and the evolution of its key biochemical components are deeply intertwined with Earth's early atmospheric conditions and biogeochemical cycles. Since Miller's landmark contribution in 1953,[5] extensive research has explored the origin of prebiotic building blocks under diverse conditions.[6–10] Currently, most studies focus on synthesizing individual prebiotic molecules, while one-pot synthesis of multiple components remains a major challenge in understanding life's emergence on early Earth.

Lightning, a key driver of prebiotic chemistry on early Earth, likely provided energy for atmospheric reactions, promoting the formation of amino acids and other organic compounds, as recent studies suggest.[11–15] Furthermore, a significant portion of early Earth's surface was covered by liquid environments, where lightning strikes likely generated bubbles. This gas–liquid plasma environment could have provided a highly reactive microenvironment, promoting the synthesis of complex organic molecules.[16,17]

Based on this, plasma bubbles from lightning–sea interactions may have played a key role in prebiotic chemistry, creating a high-reactivity environment that accelerates organic molecule synthesis, similar to early Earth processes. Our previous work[18,19] demonstrated that CO_2 plasma bubbles can produce organic acids and long-chain hydrocarbons at high yields, further supporting the idea of plasma bubbles as a potential "cradle" for prebiotic molecular formation. Recent advances in electrified and plasma-assisted gas–liquid interfaces have shown that non-equilibrium microenvironments can dramatically enhance C–N coupling and molecular complexity, in both material synthesis and sustainable chemical production.[20–22] Our lightning-driven plasma bubbles represent a prebiotic analogue of such systems, where similar interface effects are harnessed to generate amino acids and nucleobases from CO_2/NH_3 mixtures.

Here we developed a plasma bubble discharge system to simulate lightning strikes on the ocean (Fig. 1A and Fig. S1, S2). By applying negative DC voltage and introducing NH_3 and CO_2, we replicated early Earth conditions. Micropores at the reactor base promote plasma bubble formation (Fig. 1B), creating an

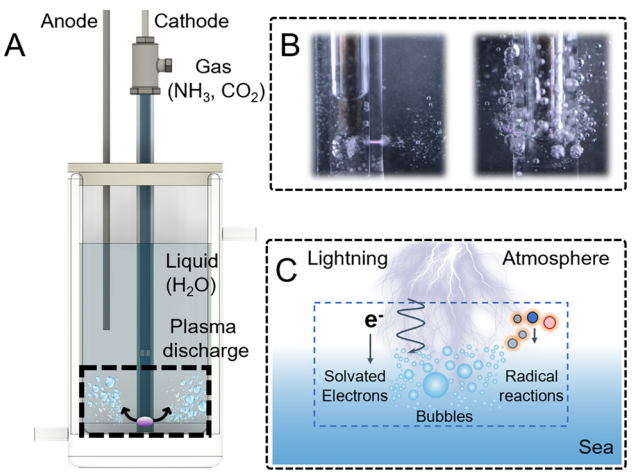

Fig. 1 (A) Schematic diagram of the plasma bubble system, designed to simulate the phenomenon of lightning striking the sea, with NH_3 and CO_2 used to represent the coexistence of oxidizing and reducing atmospheres. (B) A transient image of the plasma bubbles captured by a high-speed camera. (C) Plasma bubble chemistry induced by lightning.

[a] *State Key Laboratory of Electrical Insulation and Power Equipment, Centre for Plasma Biomedicine, Xi'an Jiaotong University, Xi'an 710049, China. E-mail: renwu.zhou@xjtu.edu.cn*
[b] *Qian Xuesen Collaborative Research Center of Astrochemistry and Space Life Sciences, Ningbo University, Ningbo 315211, China. E-mail: yingjianxi@nbu.edu.cn*
[c] *School of Chemical and Biomolecular Engineering, The University of Sydney, Sydney, New South Wales 2006, Australia. E-mail: Tianqi.zhang@sydney.edu.au*
[d] *Earth and Planets Laboratory, Carnegie Institution for Science, Washington, DC 20015, USA*

environment for prebiotic biomolecule synthesis *via* gas–liquid plasma chemistry (Fig. 1C).

J. David Felix's estimates of substantial NH_3/NH_4^+ fluxes from Archean-like hydrothermal systems[23] and the experimental demonstration by Gao *et al.* that Fe-rich rock–water interactions can efficiently generate NH_3 from nitrate together suggest that ammonia could have been locally abundant on the early Earth,[24] which motivated our use of an $NH_3/CO_2 = 1:1$ gas mixture to simulate a nitrogen-rich prebiotic atmosphere–ocean interface.

LC-MS analysis identified 12 amino acids and 3 canonical nucleobases (Fig. 2A and Fig. S3–S16, S38, Table S1). MS/MS analysis identified Gly–Gly, with the *m/z* of $[M + H]^+$ 133.0608 and Gly diketopiperazine (DKP), with the *m/z* of $[M + H]^+$ 115.0503 (Fig. 2B), suggesting that under early Earth conditions, plasma bubbles could facilitate the formation of amino acids, peptides, and cyclic peptides. This one-pot reaction, producing 12 amino acids, peptides, DKP, and three nucleobases, is unprecedented. To evaluate how early Earth conditions affected prebiotic synthesis, we systematically analysed the impact of lightning discharge intensity and gas flow rate on biomolecule production (Table S2). Notably, the gas flow rate governs the size of bubbles in the discharge reactor (Fig. S17). Smaller micro- and nano-bubbles provide a greater interfacial area and longer lifetime, enhancing the generation of reactive species. Recent studies on electrospark-induced bubble rupture confirm that discharge fragmentation produces micro/nano-bubbles that act as highly efficient electrochemical micro-reactors.[25] The promoting effect is therefore most pronounced for bubbles ~100 μm in diameter. With quantitative analysis performed using standard concentration curves (Fig. S18–S21), the observed concentration gradient (Gly, 0.4 nM > Ala, 0.15 nM > Asn, 0. 04 nM > Glu, 0.02 nM) suggests preferential formation of smaller, less polar amino acids under the simulated early Earth conditions. We also assessed the effect of varying voltages (3–5 kV) on product formation, finding minimal impact on the synthesis of the same product (Table S2). And it was found that the discharge temperature at different voltages increased proportionally with time (Fig. S22). Further research has shown that the yield of Gly decreased continuously as the concentration of NH_3 decreased, revealing that the NH_3-rich condition is important for amino acid formation (Fig. S23). This might be because NH_3 can provide a reducing environment, which is of great significance for the chemical synthesis of life molecules. The emergence of life likely involved the interaction and symbiosis of various molecular species, rather than the evolution of a single substance, the simultaneous synthesis of multiple amino acids and nucleobases under these conditions provides a key insight into the molecular interactions that may have driven the co-evolution of life's building blocks.[26–29]

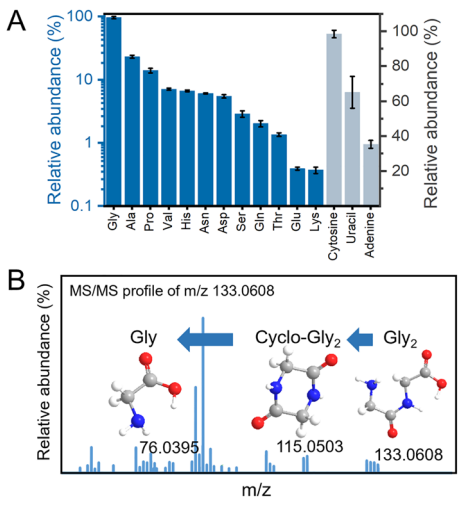

Fig. 2 Products analyzed after plasma discharge. The bar heights are derived from the same relative LC–MS signal categories as Table S2 (after normalization), ensuring a consistent use of "relative intensity" throughout. (A) Relative abundance of the amino acids and nucleobases produced in the plasma bubble system. For the same type of product (amino acid or nucleobase), the product with the highest signal strength in that type after discharge is set to 1. (B) MS/MS profile of the solution after discharge, verifying the formation of Gly_2, cyclo-Gly_2 and Gly.

To highlight the superiority of plasma bubbles in synthesizing life-building blocks, we compared them with needle plasma discharge environments, both plausible in lightning scenarios. Fig. S24 shows that plasma bubbles significantly outperform needle plasma in product formation, with glycine levels more than three times higher in bubble plasma. This enhancement is likely due to spark discharges within gas bubbles, providing a large surface area and promoting efficient NH_3–CO_2 reactions. Our previous work demonstrates that plasma bubbles create an optimal gas–liquid interface, enhancing the generation and transfer of active particles.[30,31]

The emergence of biomolecules from non-living matter has long been a research focus. However, the direct transition from inorganic gases to functional peptides or cyclic peptides (*e.g.*, cyclic-Gly_2) remains rare. Here we demonstrate the prebiotic synthesis of dipeptides and cyclic dipeptides from inorganic gases and explore the reactivity of the 20 proteinogenic amino acids in a plasma bubble environment, proposing a novel pathway for amino acid conversion to polypeptides on early Earth. Furthermore, we explored the reactivity of amino acids in the plasma bubble system. As shown in Fig. 3, 106 dipeptides were detected, with amino acids such as Gly, Leu, Val, Gln, and Ile—likely present on early Earth—forming the corresponding dipeptides. Higher-order peptides, including a hexamer (Gly_6) (Fig. S25), were also observed. These results highlight the plasma bubble system's role in the study of life's molecular origins, particularly in polypeptide formation.

To further explore the reaction mechanism, we first utilized optical emission spectroscopy (OES) to detect the reactive species during the underwater discharge process of (CO_2/NH_3) gas bubbles. The results are presented in Fig. 4A. The results showed that excited hydroxyl (OH) radicals, atomic oxygen (O), and H radicals were generated in CO_2/NH_3 plasmas. The formation of OH emissions from the transition of $A^2\Sigma^+ \rightarrow X^2\Pi$ ($\Delta\nu = 0$) at 309 nm and H_α emissions at 656 nm mainly comes from the electron impact dissociations ($H_2O + e^- \rightarrow H + OH + e^-$) at the plasma–water interface.[32] The O emission at

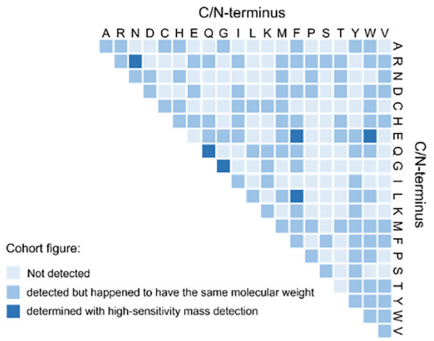

Fig. 3 Profile of the detected possible dipeptides through bubble and Ar plasma starting from a 20 amino acid mixture (deep blue = determined with high-sensitivity mass detection, blue = detected by HR-MS but sharing the same molecular weight with other possible isomers (isobaric dipeptides) and therefore not individually confirmed by MS/MS, light blue = not detected). Amino acids are indicated according to the one-letter abbreviation.

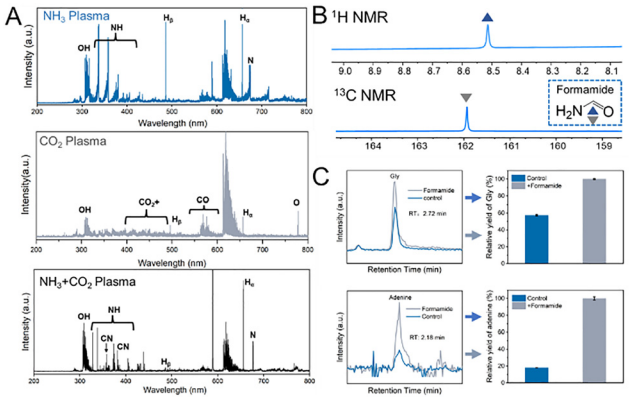

Fig. 4 Mechanism Exploration. (A) Optical emission spectrum of the NH_3/CO_2 plasma discharge. (B) ^{1}H NMR and ^{13}C NMR profile of the solution after discharge, verifying the formation of formamide. (C) The influence of formamide addition on the prebiotic building blocks formation.

777 nm, corresponding to the oxygen atom transition of O ($2s^2 2p^3 3s$–$2s^2 sp^3 3p$), was visible due to the energetic collisions of electrons with H_2O molecules ($H_2O + e^- \rightarrow 2H + O + e^-$).[33] In addition, it shows different bands indicating the various reactions and excitation substances produced during the decomposition of CO_2 and NH_3 in the plasma environment. For CO_2 plasma discharge, the emission spectra show significant electronic transitions of the CO_2^+ and CO Angstrom band, which are key intermediates in plasma-induced CO_2 decomposition reactions.[34] Among them, CO may play an important role in the subsequent formation of reactive molecules in the reaction process. For NH_3 plasma discharge, the characteristic emission peaks of the NH group were observed between 330 and 400 nm, indicating that NH_3 underwent dissociation, which is related to the electronic excitation and recombination of the nitrogen–hydrogen bonds.[35] Notably, the CN radical was observed at 359 nm and 388 nm, indicating the coupling of CO_2 and NH_3. The CN species could play an important role in the subsequent plasma synthesis of nucleobases.[36]

Formamide formation was confirmed *via* NMR and GC-MS (Fig. 4B and Fig. S26), suggesting its role as a key precursor for amino acid and nucleobase synthesis, as proposed by Ferus, Bada, and Saitta *et al.* To investigate the chemical pathways of formamide synthesis and its role in amino acid and nucleobase formation, DFT calculations and chemical kinetic simulations were combined with experimental results. Product synthesis was most efficient at the gas–liquid interface (discharge at the bubble–water interface), as compared to needle plasma discharge (Fig. 2C). We propose the following reaction pathways: (i) CO_2 dissociation forms CO and O (Fig. 4A); (ii) CO reacts with OH and H from H_2O dissociation to form formic acid (HCOOH) (Fig. S27); (iii) HCOOH then reacts with NH_2 radicals to form formamide ($HCONH_2$) (Fig. 4B); (iv) Amino acids and canonical nucleobases are subsequently generated from formamide. DFT calculations show that CO reacts with H_2O, overcoming a 30 kcal mol^{-1} energy barrier, while HCOOH formed from CO and H_2O reacts with NH_3 to overcome a 59 kcal mol^{-1} barrier, predicting fast kinetics under plasma bubble discharge conditions (Fig. S28).

Based on these findings, we propose a chemical mechanism for converting inorganic gases into prebiotic building blocks in a plasma bubble environment (Fig. 5). The reaction kinetics in the NH_3–CO_2 plasma bubble system reveal formamide ($HCONH_2$) as a key prebiotic intermediate, with its formation occurring in two phases. During the rapid formation phase (0–0.4 s), high fluxes of radicals and small molecules drive formamide synthesis through CO–NH_3 coupling and a HCOOH-derived pathway. Formamide concentration peaks at $\sim 10^{-8}$–10^{-12} cm^{-3} before declining due to hydrolysis and competition from nitrogenous by-products. Formamide's transient accumulation highlights its potential as a precursor for nucleobases and amino acids (Fig. 5C and D).[37,38] For example, amino acids *via* Strecker synthesis, consistent with the amino nitrile species observed in our mass spectrometry analysis (Fig. S29–S34), additional experiment (Fig. S35) and previous reports,[39–41] further confirmed the reaction pathway, supporting lightning-induced reactive environments as plausible drivers of early biomolecular synthesis. These amino acids can then further polymerize to form peptides, as demonstrated in this study. Regarding nucleobases, formamide dissociates to generate CN, which subsequently undergoes a series of reactions to form nucleobases, with uracil being derived from cytosine.[42] Taken together with previous studies,[43–45] our results highlight the key role of formamide in prebiotic chemistry: in the plasma-bubble system, it serves both as a direct precursor to nucleobases and other organics and as a transient reservoir of C–N species in a lightning-activated CO_2/NH_3 atmosphere–ocean setting. All of the above underscores the role of non-equilibrium plasma dynamics, where transient radical fluxes and competing pathways govern the synthesis and stability of life's building blocks.

In summary, the abiotic origin of life's molecular precursors on early Earth necessitates efficient pathways for biomolecule synthesis and polymerization. This study shows that lightning-induced plasma bubbles serve as high-energy geochemical

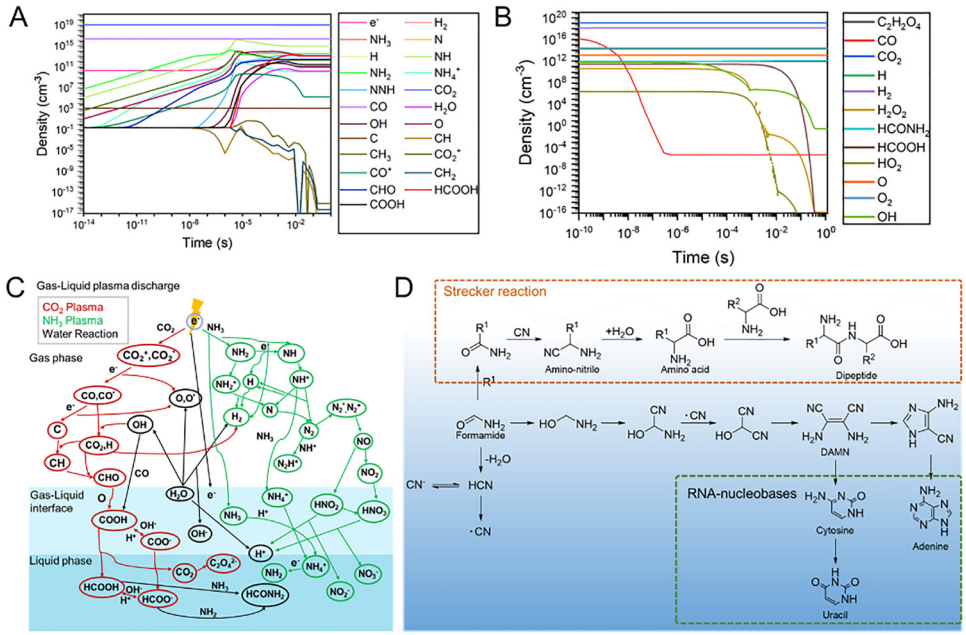

Fig. 5 The mechanism of prebiotic chemistry in the plasma bubble. Density profiles of important (A) gas phase and (B) aqueous phase species, showed that the three key species ($C_2H_2O_4$, HCOOH and $HCONH_2$) exhibit a decreasing trend. (C) Plasma discharge chemistry under the gas–liquid conditions, from NH_3 and CO_2 to the formamide. (D) The reactions from formamide to prebiotic building blocks; the pathways shown in the figure are either confirmed in this study or are based on previous literature reports.[1–4]

reactors, enabling rapid synthesis of amino acids (12 types), RNA nucleobases (3 types), urea, biuret (Fig. S36 and S37) and oligopeptides at gas–liquid interfaces. Simulated plasma discharges in NH_3/CO_2 atmospheres generate reactive nitrogen and carbon species (*e.g.*, CN, NH_2, CO), driving formamide-mediated Strecker synthesis and HCN oligomerization. These processes produce biomolecules within minutes, surpassing conventional methods (Table S3). By bypassing thermodynamic barriers *via* non-equilibrium plasma excitation, the system concurrently synthesizes nucleobases and amino acids. This plasma-mediated pathway completes a critical biogeochemical cycle, converting atmospheric CO_2 and NH_3 into bioavailable organic compounds. Whilst such high abundances of NH_3 may not have been uniformly present in primordial Earth's atmosphere, geochemical and photochemical flux studies indicate that substantial local or episodic NH_3 inputs were plausible, thereby supporting the relevance of investigating NH_3/CO_2 mixtures. In this context, our 1 : 1 NH_3/CO_2 mixture should be interpreted as a model system to probe fundamental plasma-driven prebiotic chemistry. Moreover, ammonia-rich settings have been widely proposed for several icy bodies in the outer solar system—including Enceladus, Titan, Triton, and Pluto—where NH_3–H_2O or NH_3–CO_2–H_2O ices and vapour phases are thought to have co-existed. Observational, experimental, and thermochemical modelling studies provide substantial evidence for the presence and chemical importance of ammonia in these environments.[46–48] In this broader astrochemical context, our 1 : 1 NH_3/CO_2 mixture is therefore best interpreted as a model system designed to probe fundamental plasma-driven nitrogen–carbon coupling chemistry. The identified mechanism positions atmospheric electrical discharges as a key driver in early Earth's surface–atmosphere exchanges, complementing existing prebiotic synthesis paradigms.

Conflicts of interest

There are no conflicts to declare.

Data availability

All data of this study are included in this published article and its supplementary information (SI). Supplementary information is available. See DOI: https://doi.org/10.1039/d5cc04325e.

Acknowledgements

This work is supported by the National Natural Science Foundation of China (524B2109, 52377160, GYKP010, and 42388101) and the Shaanxi Provincial Natural Science Program (2023-JC-YB-425).

References

1 S. Miyakawa, K. Kobayashi and A. B. Sawaoka, *Adv. Space Res.*, 1999, **24**, 465–468.
2 A. Pastorek, J. Hrnčířová, L. Jankovič, L. Nejdl, S. Civiš, O. Ivanek, V. Shestivska, A. Knížek, P. Kubelík, J. Šponer, L. Petera, A. Křivková, G. Cassone, M. Vaculovičová, J. E. Šponer and M. Ferus, *Chem. Commun.*, 2019, **55**, 10563–10566.
3 M. Yadav, R. Kumar and R. Krishnamurthy, *Chem. Rev.*, 2020, **120**, 4766–4805.
4 M. Ferus, F. Pietrucci, A. M. Saitta, O. Ivanek, A. Knizek, P. Kubelík, M. Krus, L. Juha, R. Dudzak, J. Dostál, A. Pastorek, L. Petera, J. Hrncirova, H. Saeidfirozeh, V. Shestivská, J. Sponer, J. E. Sponer,

P. Rimmer, S. Civiš and G. J. A. Cassone, *Astron. Astrophys.*, 2019, **626**, A52.
5 S. L. Miller, *Science*, 1953, **117**, 528–529.
6 H. James CleavesII, A. M. Scott, F. C. Hill, J. Leszczynski, N. Sahai and R. Hazen, *Chem. Soc. Rev.*, 2012, **41**, 5502–5525.
7 D. W. Gan, Y. T. Guo, X. M. Lei, M. Zhang, S. S. Fu, J. X. Ying and Y. F. Zhao, *Earth Planet. Sci. Lett.*, 2023, **607**, 118072.
8 L. Zhang, M. Zhang, X. F. Guo, D. W. Gan, Y. Ye, Y. F. Zhao and J. X. Ying, *Chem. Commun.*, 2024, **60**, 2748–2751.
9 Z. R. Todd, R. Szabla, J. W. Szostak and D. D. Sasselov, *Chem. Commun.*, 2019, **55**, 10388–10391.
10 A. Pastorek, J. Hrnčířová, L. Jankovič, L. Nejdl, S. Civiš, O. Ivanek, V. Shestivska, A. Knížek, P. Kubelík, J. Šponer, L. Petera, A. Křivková, G. Cassone, M. Vaculovičová, J. E. Šponer and M. Ferus, *Chem. Commun.*, 2019, **55**, 10563–10566.
11 B. L. Hess, S. Piazolo and J. Harvey, *Nat. Commun.*, 2021, **12**, 1535.
12 M. Ferus, F. Pietrucci, A. M. Saitta, O. Ivanek, A. Knizek, P. Kubelík, M. Krus, L. Juha, R. Dudzak and J. Dostál, *Astron. Astrophys.*, 2019, **626**, A52.
13 K. Kobayashi and P. Cyril, *Origins Life Evol. Biospheres*, 1985, **16**, 57–67.
14 X. F. Xiang, L. Guo, X. Wu, X. X. Ma and Y. S. Xia, *Environ. Chem. Lett.*, 2012, **10**, 295–300.
15 C. R. Stark, C. Helling, D. A. Diver and P. B. Rimmer, *Int. J. Astrobiol.*, 2014, **13**, 165–172.
16 E. Tekin, A. Salditt, P. Schwintek, S. Wunnava, J. Langlais, J. Saenz, D. Tang, P. Schwille, C. Mast and D. Braun, *ChemBioChem*, 2022, **23**, e202200423.
17 N. Ben-Amots and M. Anbar, *Ultrason. Sonochem.*, 2007, **14**, 672–675.
18 T. Q. Zhang, J. Knezevic, M. Y. Zhu, J. M. Hong, R. S. Zhou, Q. Song, L. Y. Ding, J. Sun, D. X. Liu, K. K. Ostrikov, R. W. Zhou and P. J. Cullen, *J. Am. Chem. Soc.*, 2023, **145**, 28233–28239.
19 J. Knezevic, T. Q. Zhang, R. W. Zhou, J. M. Hong, R. S. Zhou, C. Barnett, Q. Song, Y. T. Gao, W. P. Xu, D. X. Liu, N. Proschogo, B. Mohanty, J. Strachan, B. Soltani, F. Li, T. Maschmeyer, E. C. Lovell and P. J. Cullen, *J. Am. Chem. Soc.*, 2024, **146**, 12601–12608.
20 D. Li, Y. Zhao, Y. Miao, C. Zhou, L. P. Zhang, L. Z. Wu and T. Zhang, *Adv. Mater.*, 2022, **34**, e2207793.
21 Y. Zhao, Y. Zhao, G. I. N. Waterhouse, L. Zheng, X. Cao, F. Teng, L. Z. Wu, C. H. Tung, D. O'Hare and T. Zhang, *Adv. Mater.*, 2017, **29**, 1703828.
22 Y. Wang, Y. Liu, J. Gan, L. Hong, J. Shen, Z. Zhang, H. Zheng and X. Wang, *ACS Sustainable Chem. Eng.*, 2024, **12**, 14505–14513.
23 J. D. Felix, *Sci. Rep.*, 2024, **14**, 1544.
24 Y. Gao, M. Lei, B. Sravan Kumar, H. B. Smith, S. H. Han, L. Sangabattula, J. Li and I. I. Abate, *Joule*, 2025, **9**, 101805.
25 M. Zhu, M. Zhang, X. Wang, C. Liu, R. Zhou, J. Sun, R. Zhou and D. Liu, *J. Phys. Chem. Lett.*, 2025, **16**, 11101–11108.
26 M. Frenkel-Pinter, M. Samanta, G. Ashkenasy and L. J. Leman, *Chem. Rev.*, 2020, **120**, 4707–4765.
27 C. J. Butch, M. Meringer, J.-S. Gagnon and H. J. Cleaves, *Commun. Chem.*, 2021, **4**, 11.
28 S. Tagami, J. Attwater and P. Holliger, *Nat. Chem.*, 2017, **9**, 325–332.
29 S. Chatterjee, *Phys. Chem. Chem. Phys.*, 2016, **18**, 20033–20046.
30 D. W. Gan, J. W. Huang, L. F. Hong, H. X. Jiang, X. R. Wang, R. S. Zhou, J. Sun and R. W. Zhou, *Green Chem.*, 2025, **27**, 8811–8817.
31 D. W. Gan, L. F. Hong, S. Yuan, M. Y. Zhu, Y. T. Gao, T. Q. Zhang, T. Y. Li, B. H. Chen, A. Dzimitrowicz, P. Jamroz, P. J. Cullen and R. Zhou, *Green Chem.*, 2025, **27**, 3715–3726.
32 S. Wang, D.-Z. Yang, R. S. Zhou, R. W. Zhou, Z. Fang, W. C. Wang and K. Ostrikov, *Plasma Processes Polym.*, 2020, **17**, 1900146.
33 X. Lu, G. V. Naidis, M. Laroussi, S. Reuter, D. B. Graves and K. Ostrikov, *Phys. Rep.*, 2016, **630**, 1–84.
34 Y. J. Du, K. Tamura, S. Moore, Z. M. Peng, T. Nozaki and P. J. Bruggeman, *Plasma Chem. Plasma Process.*, 2017, **37**, 29–41.
35 U. Müller and G. Schulz, *J. Chem. Phys.*, 1992, **96**, 5924–5937.
36 M. Ferus, D. Nesvorný, J. Šponer, P. Kubelík, R. Michalčíková, V. Shestivská, J. E. Šponer and S. Civiš, *Proc. Natl. Acad. Sci. U. S. A.*, 2015, **112**, 657–662.
37 D. Deamer, *J. Mol. Evol.*, 2024, **92**, 530–538.
38 A. S. Burton, J. C. Stern, J. E. Elsila, D. P. Glavin and J. P. Dworkin, *Chem. Soc. Rev.*, 2012, **41**, 5459–5472.
39 N. J. Green, D. A. Russell, S. H. Tanner and J. D. Sutherland, *J. Am. Chem. Soc.*, 2023, **145**, 10533–10541.
40 K. K. Farnsworth, H. L. McLain, A. Chung and M. G. Trainer, *ACS Earth Space Chem.*, 2024, **8**, 2380–2392.
41 K. Ashe, C. Fernández-García, M. K. Corpinot, A. J. Coggins, D.-K. Bučar and M. W. Powner, *Commun. Chem.*, 2019, **2**, 23.
42 M. Yadav, R. Kumar and R. Krishnamurthy, *Chem. Rev.*, 2020, **120**, 4766–4805.
43 R. Saladino, E. Di Mauro and J. M. García-Ruiz, *Chemistry*, 2019, **25**, 3181–3189.
44 R. Saladino, C. Crestini, F. Ciciriello, G. Costanzo and E. Di Mauro, *Chem. Biodiversity*, 2007, **4**, 694–720.
45 R. Saladino, C. Crestini, S. Pino, G. Costanzo and E. Di Mauro, *Phys. Life Rev.*, 2012, **9**, 84–104.
46 M. Nasralla, H. Laurent, O. L. G. Alderman and L. Dougan, *Commun. Chem.*, 2025, **8**, 227.
47 G. M. Marion, J. S. Kargel, D. C. Catling and J. I. Lunine, *Icarus*, 2012, **220**, 932–946.
48 W. Zheng, D. Jewitt and R. I. Kaiser, *Astrophys. J., Suppl. Ser.*, 2009, **181**, 53.

